Rev.Adv.Mater.Sci. 10 (2005) 447-453

CHARACTERIZATION OF THE VISCOPLASTIC BEHAVIOR OF NANOCRYSTALLINE METALS AT HCV DEFORMATION

Lembit Kommel[1], Irina Hussainova[1] and Rainer Traksmaa[2]

[1]Department of Materials Engineering, Tallinn University of Technology Ehitajate tee 5, 19086 Tallinn, Estonia
[2]Centre for Materials Research, Tallinn University of Technology Ehitajate tee 5, 19086 Tallinn, Estonia

Received: May 04 2005; in revised form: July 20, 2005

Abstract. Viscoplastic behavior of pure nanocrystalline (NC) copper subjected to a hard cyclic viscoplastic (HCV) deformation has been studied at the present work. Test specimens were fabricated by the severe plastic deformation (SPD) technique using the equal-channel angular pressing (ECAP) method. Structural features and mechanical properties of NC copper were analyzed after the HCV treatment. Material properties and structure are shown to be influenced by heating and deformation to a great extend. For comparison, behavior of ultra-fine grained (UFG) and coarse-grained (CG) copper under the similar conditions is presented.

1. INTRODUCTION

It is well known [1,2] that the severe plastic deformation (SPD) technique of the equal channel angular pressing (ECAP) method can be used to fabricate ultrafine grained (100 – 1000 nm) or nanocrystalline (under 100 nm) metallic materials. It has been established that at the simple shear stress SPD causes a decrease in the grain size and an enhancement of mechanical properties [3-6]. The data available from the published studies, for example [7-9], show a significant scatter in the values of the mechanical properties of pure copper depending on the structural features. In contrast to many materials, nanostructured copper possesses both relative high strength and ductility resulting from an appropriate heat treatment [10]. A theoretical model is used in [11] to describe the hardening-softening mechanisms of NC metals under high-strain-rate superplastic deformation. Plastic deformation and strain hardening mechanisms are discussed in [12,13]. To understand a materials behavior its hardening-softening mechanism under cyclic deformation, the evolution of the microstructure and the true stresses at fracture are essential to know [14-16]. To investigate the viscoplastic behavior of materials, the nondestructive experimental HCV deformation [10] method proposed by the authors can be applied.

In this study, the tension test (up to total fracture) of HCV deformed specimens was performed to analyze the fracture mode depending on the structure states of the metal before and after of tensile testing. The main aims of this paper are, to study (i) the viscoplastic behavior of pure copper and (ii) the

Corresponding author: Lembit Kommel, e-mail: kommel@edu.ttu.ee

microstructure evolution and (iii) changing of the mechanical properties of materials subjected to HCV deformation.

2. MATERIALS AND EXPERIMENTAL PROCEDURES

To study viscoplastic behavior, technically pure copper (0.0238 Fe, 0.0084 Al, and balance – Cu) was chosen as a model material. Detailed ECAP procedure is described elsewhere [3,4]. A special die containing two channels of equal cross–section intersected at an angle of Φ=90° was used for ECA pressing. Cylindrical specimens subjected to SPD were prepared from pure annealed copper bars of 16 mm in diameter and 150 mm length. Each ECA pressing was conducted in air at room temperature under velocity 5 mm·s^{-1}, following 'route B_C' [2,3]. During ECAP, the compression stress of around 150 –165 MPa was applied. The material was subjected to eleven ECAP passes. After SPD the samples were subjected to HCV deformation without subsequent heat treatment (Sample N1), with heat treatment up to 200 °C with a heating rate of 1 °C·min^{-1} (N2) and with double heat treatment up to 400 °C with a heating rate of 2 °C·min^{-1} (N3). For comparison, the cold-drawn copper (N4) and the annealed at 650 °C for 1.5 h copper (N5), both of CG structure state, were used. All these samples (N1–N5) were subjected to HCV deformation. As reference materials the annealed CG copper (N6) and NC copper (N7), which were not HCV deformed, were subjected to tension up to total fracture. Samples for testing were manufactured by turning. The tension sample test part geometry has distance of 30 mm between shoulders and of 10±0.05 mm diameter with a fillet radius of 3 mm. This test part was mechanically polished to remove a damaged layer from a surface. The HCV deformation and subsequent tension were performed with the Materials Testing System INSTRON 8516. Specimens were stressed at tension-compression cycles in a viscoplastic state under axial strain in three regimes: 1 – under 1% of strain amplitude; 2 – under 2% of strain amplitude (these specimens were preliminarily strained at amplitude of 1% as in the first regime); 3 – under 1% of strain amplitude (the specimens deformed in the first two regimes were used). Tests were conducted under the strain control regime and 30 cycles during 600 s were performed at each regime. Strain amplitude was measured by the extensometer with the base length of 25 mm. Tensile straining up to total fracture was applied to the specimens at room temperature of around 23 °C and humidity of 40% at the sample rate of 3.0 pts·s^{-1} and the ramp rate of 0.03 mm·s^{-1}.

The structure of materials was studied by means of the scanning electron microscope (SEM) Gemini, LEO, Supra 35. The Bruker Analytical X-ray System Diffractometer D5005 and the WIN-CRYSIZE program were used for estimation a crystallite size of materials and microstrains inside crystallites relatively to LaB_6 sample. Mechanical properties were measured by help of the universal hardness tester Zwick Z2.5/TS1S, using the micro-indentation method according to the EVS-EN ISO 14577-1:2003 standard.

3. RESULTS AND DISCUSSION

The hysteresis loops of HCV deformation are shown in Fig. 1. There are four stress-strain loops, characterizing the main hardening-softening modes: a – softening during tension and hardening during compression cycles (N1, regime 1), b – with stable stress amplitude (N2, regime 3), c – hardening only (N3, regime 1) and d – softening only (N4, regime 1). The maximal values of stress amplitude under tension and compression cycle the specimens are presented in Fig. 1e. The viscoplastic behavior of NC copper (N1) during HCV deformation was analyzed. During the very first tensile loading after 10 s, the ultimate stress for the specimen N1 was about σ_1 = 430 MPa and during 11 cycles it rapidly decreased down to σ_{11} = 375.9 MPa or at 12.5%. At the same time, during the first compressive loading, the maximal compressing stress was only σ_{-1} = 297 MPa and during 11 cycles it rapidly increased up to σ_{-11} = 332 MPa. At the end of testing under conditions of regime 1, the ultimate tensile stress was changed down to σ_{30} = 347 MPa and the compressing stress up to σ_{-30} = 344 MPa. This phenomenon during the very first tension-compression cycle was repeated during testing according to regime 2 and regime 3, when strain amplitude was 2% and 1 % (Fig. 1d, curves N1T-tension and N1C-compression). Applying regime 2, it was found that the ultimate tensile stress decreases during the several initial cycles from σ_{31} = 418 to σ_{33} = 405 MPa and then decreases to σ_{60} = 371 MPa. During the compression, the maximum value of compressing stress σ_{-33} = 409 MPa was received after 3-4 cycles. After some cycles the compressing stress was very slowly decreased down to σ_{-41} = 401 MPa and then to σ_{-60} = 379 MPa after 60 cycles. The ultimate tensile stress at the first cycle under regime 3 was decreased to σ_{61} = 344 MPa and the compressing stress to σ_{-61} = 301 MPa. Finally, the ultimate tensile stress was

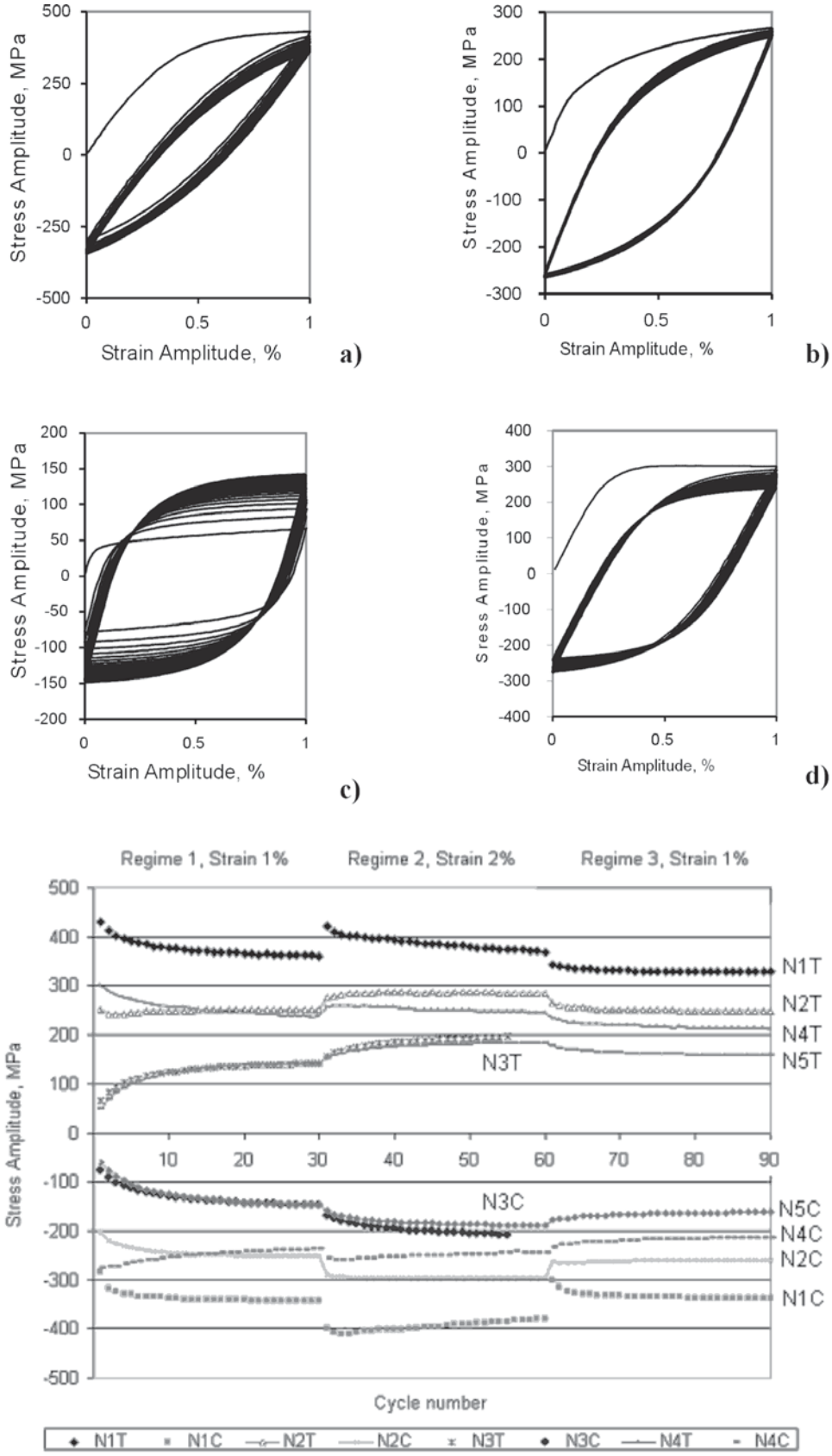

Fig. 1. Typical hysteresis loops of the stress-strain amplitude: a – NC copper (N1) softening by tension and hardening by compression cycle, b – small softening at tension cycles (during regime 3) of NC heat-treated copper (N2), c – hardening behavior of UFG (double heat-treated NC) copper (N3), d – softening behavior of cold-drawn CG copper (N4) and e – maximal values of stress at tension and stress at compression for all specimens during HCV deformation at three regimes.

decreased to σ_{90} = 328 MPa and the compressing stress to σ_{-90} = 337 MPa.

The heat treated NC copper (N2) showed a very stable stress amplitude (Fig. 1b). The annealed CG (N5) and UFG (N3) copper showed hardening behavior during regimes 1 and 2. During cyclic loading the softening behavior take place at regime 3 (Fig. 1e, curves N5T and N5C). Figs. 1d and 1e present such kind of softening of CG cold-draws copper (N4). The HCV deformation refers to the phenomenon of copper strengthening-softening behavior. The differences in tensile stress at the very first cycles between NC copper N1 and CG copper N5 decrease from 400 MPa to 180 MPa by the end of testing, Fig. 1e. This behavior depends on the initial microstructure of the metal.

3.1. Tensile testing

After HCV deformation, the specimens were subjected to tensile loading. Some mechanical properties of the specimens are listed in Table 1. For comparison, the non-deformed by HCV deformation specimens of GC copper (N6) (annealed at 650 °C for 1.5 h) and NC copper (N7) (after ECAP of 11 passes) were also tensile tested.

The NC copper (N1) has maximal stress values but does not reveal strain hardening during tension. Because of this N1 material possesses the lower stress at peak (as compared with NC copper N7, presented in Table 1), as well. However NC copper after HCV deformation (N1) has little higher percent strain at peak by identical values of energy to break point at fracture. Specimen N5 has a minimal ultimate tensile strength of 216 MPa at peak point. Stress at 0.2% yield (engineering yield stress) and the Young's modulus are minimal for the CG HCV deformed copper (N5). However, its elongation to break is the largest (over 61%) one. For comparison, the annealed CG without HCV deformation (N6) has approximately similar tensile properties. Annealed UFG copper (N3) shows a maximum increase in ultimate tensile stress that gives evidence of the strain hardening of copper during tensile loading. During tension the cold-drawn state CG copper (N4) revealed the lowest energy to the break point. ECAP increases the ultimate tensile stress of the material N7 up to 430 MPa. The price of this enhancement in strength is the reduction in the ductility of the metal. The low ductility of SPD-materials is related to the fast development of the macro localization of deformation in tensile specimens [2]. This process can be suppressed by low temperature annealing. Heat treatment at a low heating rate (1 °C·min^{-1} up to 200 °C) leads to an increase in the mean crystallite size from 40 to 72 nm for NC copper (N2). However, this influences the value of the maximum ultimate tensile stress, which is decreased from 430 to 300 MPa or for 33% from the maximum strength value between N1 and N2. The percentage of strain at break (Table 1) increases from 26% to 50% (N1 and N3). The true stress at the break of a specimen (N2) increases up to 1650 MPa (defined as the true load divided by the instantaneous cross-sectional area over which the neck formation occurs). The double heat-treated specimen (N3) has the highest strain hardening in tension up to the stress of 239 MPa, and the percent of strain at the total fracture increases up to 50%. Heat treatment up to 200 °C (N2) and double treatment up to 400 °C (N3) allow for some recrystallization process passing and grain growth during coagulation process (Fig. 2b). The metal becomes softer but more ductile (Table 1), and for example, the stability of viscoplastic properties of a NC metal (N2) increases significantly (Fig. 1e, curves N2T and N2C).

3.2. Fracture mechanism

Fracture mechanism depends on the structural features of the specimen subjected to different loading. The fracture modes were studied by fracture surface characterization using SEM (Figs. 3a and 3b). During HCV deformation, microvoids with an average size around 1 μm are formed in the interior of the necking area (Fig. 3c). Microvoids concentration increases toward the fracture surface. However, as deformation continues, these microvoids do not enlarge to form a global crack. In the area of a flaw or a pore formed during HCV deformation, there are refined nanograins of an average grain size less than 10 nm possessing increased microstrains in metal (Figs. 3c and 3d). The microstrains increase influences mechanical properties. A new ultra-fine nanostructure is developed and it can be assumed that local mechanical properties in the near pore areas enhance and the yield stress increases. The microvoids coalescence and crack propagation from flaw to flaw is energetically inefficient. As a result, the fracture ensues by rapid propagation of a crack around the microvoids for NC copper N1 (Fig. 3a), and through the microvoids for cold-drawn state CG copper N4 (Fig. 3b). The present of microvoids at the stage before fracture results in decrease in Young's modulus and an increase in the true stress (Table 1).

Table 1. Mechanical properties of the specimens subjected to tensile loading.

NN	Stress at 0.05% Yield, MPa	Stress at 0.2% Yield, MPa	Stress at Peak, MPa	Percent Strain at Peak	Percent Strain at Break	True Stress at Break, MPa	Young's Modulus, GPa	Energy to Break Point, J
N1	177	250	365	2.4	26	719	36.58	185
N2	152	205	300	16.3	39	1650	34.55	243
N3	110	140	239	30	50	1170	34.23	250
N4	120	176	247	11	34	922	36.12	171
N5	89	124	216	35	61	1164	32.73	275
N6	-	43	211	42	69	1120	-	277
N7	-	208	430	1.8	27	660	125.4	183

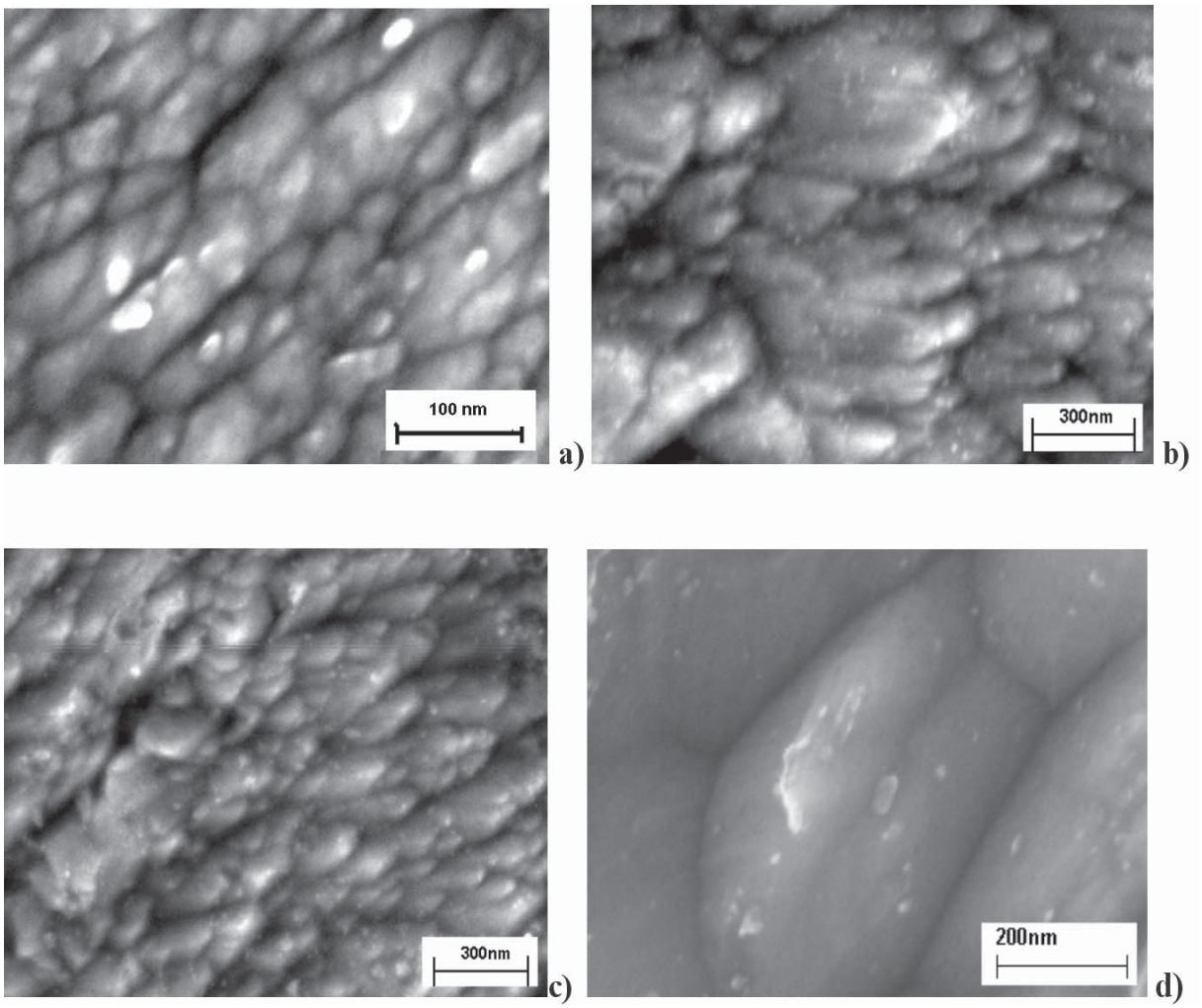

Fig. 2. SEM micrographs of NC and UFG structured copper: a – NC copper N1 after 11 passes of ECAP with oriented nanograins; b – UFG structure of copper N3 after double heat treatment (at first up to 200 °C with heating rate of 1 °C·min^{-1} and double up to 400 °C with heating rate of 2 °C·min^{-1}) with coagulated nanograins with size of 300-400 nm; c – UFG copper N3 after HCV deformation in the necking region with refining of large grains; d – nanograins joining during HCV deformation.

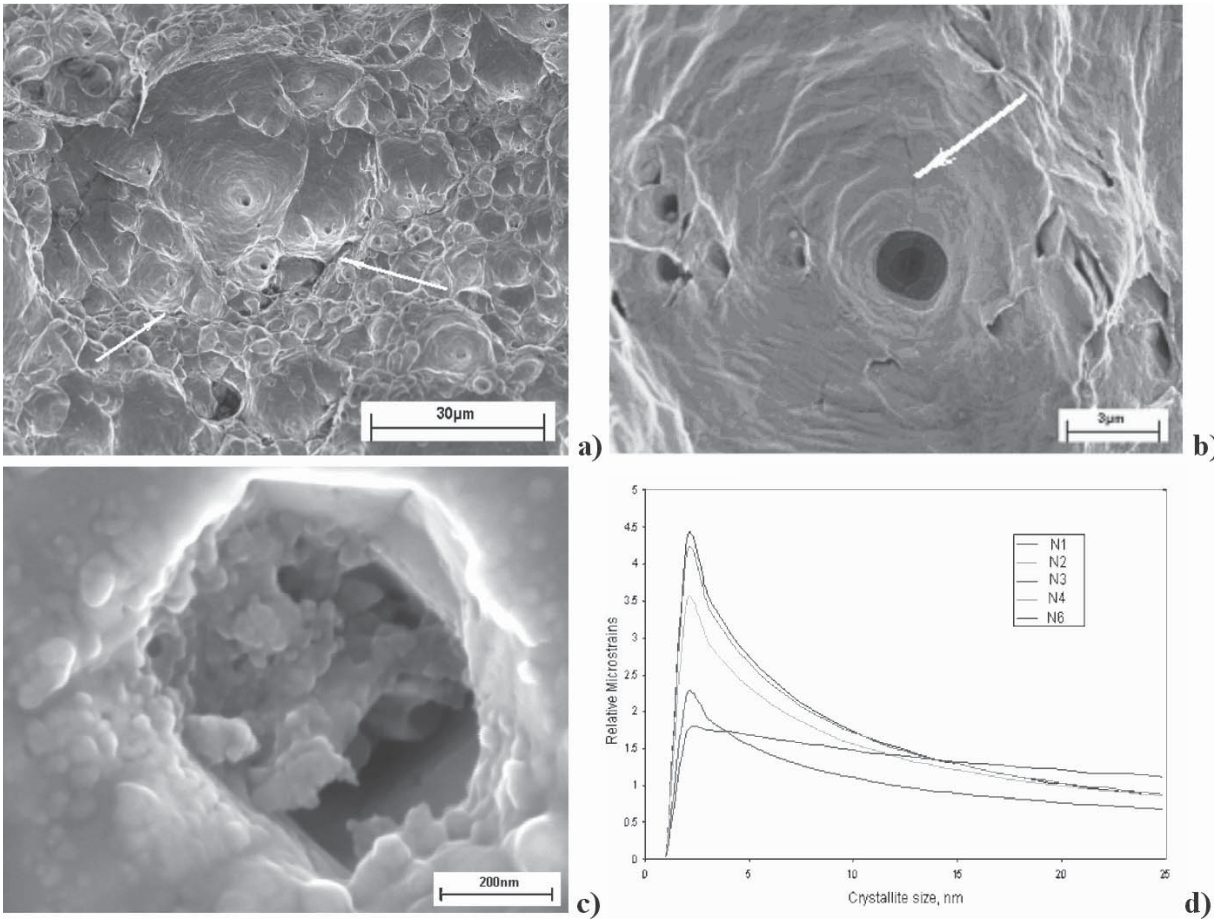

Fig. 3. Fracture surface of tension specimens: a – NC copper N1 and b – CG cold-drawn copper N4 (crack propagation is shown); c – in NC copper N1 formed microvoid (during HCV deformation) with refined nanograins in interior; d – relative microstrains distribution depending on crystallite size.

3.3. Structural evolution

SEM micrograph of the NC copper after eleven passes of ECAP via 'route B_C' is shown in Fig. 2a. The grains are of ellipsoidal shape with a mean crystallite size of about 40 nm. Materials treated with different methods have different structural states, ranging from nanocrystalline (N1) with an average grain diameter of 40 nm to UFG (N3), with an increase in grain size from 100 nm to 300 nm (Fig. 2b) during heat-treatment and CG annealed state with a mean grain size of 250 μm. The mean crystallite size measured by the XRD technique and calculated by the computing program WIN-CRYSIZE is smaller than the grain size estimated by means of the SEM micrograph analysis. During HCV deformation of UFG copper N3, large grains were refined (Fig. 2c), while with NC copper N1, the grains and crystallites sizes were increased (Fig. 2d) due to grains joining in the coagulation process.

3.4. Viability analysis

The stress-strain amplitude (Fig. 1) reflects the materials structure (Fig. 2) and micro stresses inside crystallites (Fig. 3d). During the very first compression cycle at new strain amplitude of HCV deformation regime, the stress amplitude of NC copper was increased (curve N1C). The stress magnitude depends on the structural changes during HCV deformation (Fig. 2). X-ray investigation shows that not only the grain size determines the viscoplastic properties; these properties are determined by the level of stresses inside crystallites (Fig. 3d).

The heat-treated UFG metal (N3) and annealed CG copper N5 shows an increase in the tension-

compression stress amplitude and deformation hardening. Furthermore, HCV deformation of a CG cold-drawn structure state copper (N4) influences the decrease of the tension-compression stresses and deformation softening of the metal. The increase in the tension-compression stress amplitude for the annealed copper (N5) is due to grains refinement and in dislocations density increase similar to UFG copper (N3) (Figs. 2b and 2c).

4. CONCLUSIONS

NC copper (N1) during the tension cycle exhibits only softening behavior, while during the compression cycle at the very first cycle number drastic hardening and at the end of testing after 60-90 cycles the scanty hardening behavior.

Heat treated (up to 200 °C with heating rate of 1 °C·min^{-1}) NC copper shows stable viscoplastic properties during HCV deformation up to 90 cycles. After double heat-treatment of NC copper (up to 400 °C with a heating rate of 2°C·min^{-1}), UFG copper (N3) and annealed at the temperature of 650 °C for 1.5 h CG copper (N5) revealed approximately similar to UFG copper mechanical properties and viscoplastic behavior during the very first cycles of HCV deformation; the only exception is that the viability assessment of UFG structure copper is higher.

The annealed CG copper is found to possess the mechanical properties almost similar to those of UFG copper. However, the reliability of UFG structured copper is higher. During HCV deformation, cold-drawn CG copper (N4) showed a high level of mechanical properties (identical to N2), but during HCV deformation it show only softening behavior and low viability assessment.

The HCV deformation of NC copper influences the nanograins growth, while in GC copper N5 these features influenced grains refining. HCV deformation improves the ductility of the nanostructured copper, while the ductility of the annealed material decreases during the HCV deformation.

Therefore, understanding of material behavior at the different stages of processing may allow us to tailoring the mechanical properties and to design new materials for various applications.

ACKNOWLEDGEMENTS

Support from Estonian Science Foundation under grants G-5878 and G-6163 is appreciated.

REFERENCES

[1] V.M. Segal // *Inv. Certif. of the USSR* (1977) No. **575892**.
[2] V.M. Segal // *Mater. Sci. & Eng.* **A338** (2002) 331.
[3] V.I. Kopylov, In: *NATO Science Series 3. High Technology 80*, ed. by Terry C. Lowe and Ruslan Z. Valiev (Kluwer Academic Publishers, 2000), p. 23.
[4] L. Kommel, J. Kybarsepp, R. Veinthal and R. Traksmaa, In: *Nano-Architectured and Nanostructured Materials: Fabrication, Control and Properties*, ed. by Y. Champion and H. - J. Fecht. (WILEY-VCH Verlag GmbH & Co. KGaA, 2004), p. 27.
[5] W.M. Yin and S.H. Wang // *JOM* **January** (2005) 63.
[6] H. Conrad // *Metallurgical and Materials Transactions A* **35A** (2004) 2681.
[7] Bing Q. Han, Enrique J. Lavernia and Farghalli A. Mohamed // *Rev. Adv. Mater. Sci*. **9** (2005) 11.
[8] D. H. Lassila, Tien Shen, Bu Yang Cao and Marc A. Meyers // *Metallurgical and Materials Transactions* **A 35A** (2004) 2729.
[9] Shankar M.L. Sastry // *NATO Science Series 3. High Technology 8*0**,** ed. by Terry C. Lowe and Ruslan Z. Valiev (Kluwer Academic Publishers, 2000), p. 273.
[10] L. Kommel, In: *Ultrafine Grained Materials III*, ed. by Y.T. Zhu, T.G. Langdon, R.Z. Valiev, S.L. Semiatin, D.H. Shin and T.C. Lowe (TMS, 2004), p. 571.
[11] M.Yu. Gutkin, I.A. Ovid'ko and N. V. Skiba // *Acta Mater.* **52** (2004) 1711.
[12] P.O. Kettunen, V.-T. Kuokkala, In: *Materials Science Foundations 16-18,* ed. by M. Magini and F.H. Wöhlbier (Trans Tech Publications Ltd, Switzerland, 2003), p. 410.
[13] Y.J. Li, X.H. Zeng and W. Blum // *Acta Materialia* **52** (2004) 5009.
[14] A.Yu. Vinogradov, V.V. Stolyarov, S. Hashimoto and R.Z. Valiev // *Materials Science and Engineering* **A318** (2001) 163.
[15] V. Patlan, K. Higashi, K. Kitagawa, A. Vinogradov and M. Kawazoe // *Materials Science & Engineering* **A319-321** (2001) 587.
[16] Y. Kanenko, N. Ishikawa, A. Vinogradov and K. Kitagawa // *Scripta Materialia* **38** (1998) 1609.